POLITECNICO
MILANO 1863

DIPARTIMENTO DI MECCANICA

mecc

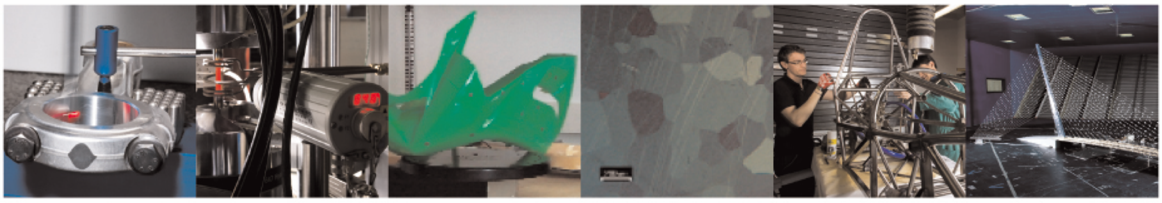

Feasibility of drone-based modal analysis using ToF-grayscale and tracking cameras

Daniele Marchisotti, Emanuele Zappa,

This is a post-peer-review, pre-copyedit version of D. Marchisotti and E. Zappa, "Feasibility of Drone-Based Modal Analysis Using ToF-Grayscale and Tracking Cameras," in IEEE *Transactions on Instrumentation and Measurement*, vol. 72, pp. 1-10, 2023, Art no. 5016210, doi: 10.1109/TIM.2023.3281628

DIPARTIMENTO DI MECCANICA ■ POLITECNICO DI MILANO
via G. La Masa, 1 ■ 20156 Milano ■ EMAIL (PEC): pecmecc@cert.polimi.it
http://www.mecc.polimi.it
Rev. 0

Feasibility of drone-based modal analysis using ToF-grayscale and tracking cameras

Daniele Marchisotti[1], Emanuele Zappa[2], *Senior Member, IEEE*

Abstract **— The application of modal analysis is a well-established procedure for detecting damage in civil structures. However, implementing monitoring systems on civil structures could involve a large number of sensors leading to expensive and cumbersome setups. On the other hand, Unmanned Aerial Vehicles (UAVs) are already employed for monitoring purposes. Moreover, by using UAVs inspections can be executed close to structures and using a single measurement node, that can be moved from one measurement point to another. In this article, a vision-based measurement procedure composed of a system mounted on a prototype drone is presented, in order to perform modal analysis of a structure. This measuring system is equipped with a grayscale camera, a Time-of-Flight (ToF) sensor and a trajectory tracking camera. This composition is necessary to measure vibrations by tracking features on the structure (grayscale camera), to convert vibrations from pixels to millimetres (ToF sensor) and to track the trajectory of the drone (trajectory tracking camera). This latter sensor is used to reduce the effect of the movement of the drone in relation to the vibrations of the structure and to reconstruct the 3D geometry of the structure. The grayscale camera on the drone is synchronized with another fixed grayscale camera, that frames a point on the structure, used as the reference point for modal analysis. This measurement procedure was tested on a mock-up of a structure a few metres in size and the results are compared with those obtained using accelerometers. The outcome of these tests proves that it is possible to correctly measure resonance frequencies (with errors lower than 0.3 %) and to reconstruct mode shapes with cameras assembled on a drone, as well as to reconstruct the 3D geometry of the points measured.**

Index Terms **— vibration measurement, drones, sensor fusion, Time-of-Flight, modal analysis**

I. Introduction

INSPECTING and monitoring structures is highly important for maintenance purposes [1]. In literature, several techniques have been investigated for executing structural health monitoring (SHM) and they are mainly divided into two categories: global and local damage identification [2]. The former is based on the assessment of the behaviour of the entire structure. The latter is particularly useful when the approximate location of a defect is known and the inspection is carried out only on a specific part of the structure [3]. In particular, local damage identification aims to detect and measure visible defects, such as concrete spalling [4] or cracks [5] in a portion of a structure, where damage is expected. On the other hand, global damage identification is meant to be applied to an entire structure, in order to identify the location of damage, that significantly modifies the modal properties. To address global damage identification, modal analysis is commonly performed using accelerometers placed on a structure and synchronized acquisition [6][7]. More recent techniques also involve the application of machine learning applied to modal analysis [8]. Nevertheless, these methods usually require training sets for machine learning and many sensors resulting in cumbersome and expensive setups that are difficult to install, although wireless sensors could be synchronized to extract modal parameters [9], with high synchronization accuracy [10] as well. At the same time, although the application of UAVs is extensively widespread for local damage identification [11] and DIC is used for modal analysis [12], the use of drones for modal analysis is investigated, since drones can be used without applying sensors to the structure, which usually requires long installation times. In addition, drones can be moved along and close to the structure to measure multiple points. Furthermore, this approach can reduce the time required to set all the instruments to a minimum, since they are mostly assembled on the drone and can be mounted a priori. However, as for the possibility of obtaining modal analysis from drone measurements is concerned, a few limitations can be present [13]. Firstly, the ability to obtain synchronized measurements of vibrations at multiple points. Secondly, a scale factor is required to convert vibrations from pixels to millimetres, the movement of the drone should not influence vibration measurements and the geometry of the structure should be known. These factors restrict the application of modal analysis using drones to small or portions of structures [13]. Furthermore, measuring vibrating targets tends to increase the uncertainty of the results [14].

In this article, a vision-based measurement procedure using sensors mounted on a drone is presented, to obtain consistent vibration data to perform modal analysis. A scheme of the procedure is visible in fig. 1.

The drone system comprises a ToF sensor, a grayscale camera and a tracking camera. The ToF sensor is used to obtain the scale factor used to convert vibration measurements from pixel units to millimetres. A pattern matching algorithm is applied to grayscale camera images to obtain vibrations in the 2D camera plane. On the other hand, the drone's trajectory is retrieved from the tracking camera in order to reduce the effect of the drone's movement on vibration measurement. This

This paper was submitted for review on February 13th, 2023. This work was partially supported by the Italian Ministry of University and Research (MIUR) in the form of the PRIN grant 2017HENS3L_003 (3DYNAMIC4.0).

[1] Daniele Marchisotti is with Politecnico di Milano, Dipartimento di Meccanica, Via La Masa 1, Milan, Italy (email: daniele.marchisotti@polimi.it)
[2] Emanuele Zappa is with Politecnico di Milano, Dipartimento di Meccanica, Via La Masa 1, Milan, Italy (email: emanuele.zappa@polimi.it)

makes it possible to pass from a drone reference system to an absolute reference system. To perform operational modal analysis, measuring of a reference point is required. This task is executed by a fixed camera.

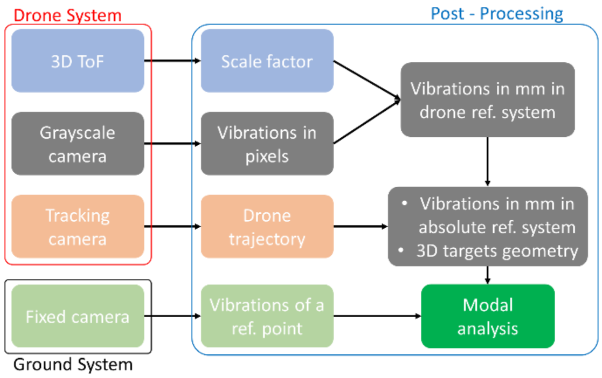

Fig. 1 – Scheme of the proposed measuring procedure

The combination of these two systems makes it possible to obtain the modal analysis of a structure, as described in Section III. In fact, the drone system is able to move in front of different parts of the structure, to measure different points of the structure (e.g. acquisition 1: points 1, 2, acquisition 2: points 3, 4, 5) and to extract vibration signals. The drone system is synchronized and calibrated, as described in Section IV. The drone system's grayscale camera is synchronized with the fixed camera, in order to calculate cross-spectra of the structure used as input for modal analysis. With this measurement procedure, the issue of synchronised measuring of different points on the structure in relation to one reference point is overcome. As a consequence, the cross-spectra between a reference point and the other points of the structure are computed for modal analysis. Furthermore, the trajectory tracking sensor is part of the drone-mounted system and it provides the points on the trajectory followed by the drone. This data, along with grayscale and ToF data, can be used to detect the position of measuring points and, therefore, the geometry of the structure (3D targets geometry, fig. 1).

The innovative parts of the proposed measurement technique presented in this article are:

1. the acquisition of vibration measurements with two synchronized and calibrated measurement systems, one on a drone and one fixed. The system on the drone is able to fly around the structure and to acquire vibrations at multiple points and these vibration data are used as input to the Operational Modal Analysis (OMA) algorithm;
2. Use of a ToF sensor to recover the pixel to millimetre scaling for each measuring point for each frame;
3. Measurement of the 3-D geometry of the structure, via the drone system, contemporarily to the vibration measurements;
4. Compensation of the movement and vibrations of the drone with the trajectory tracking sensor, to pass from a drone reference system to an absolute reference system.

The article is structured as follows. In Section II, a review of the literature on vision-based modal analysis is presented. In Section III, the proposed method is described, while in Section IV the experimental setup and validation is presented. In Section V, results from laboratory and drone tests are shown and in Section VI conclusions are drawn.

II. Related Works

Modal analysis using drones could be particularly difficult, because it requires synchronized cameras on drones or acquisition of data with overlapping of parts of the structure. For example, in [13], modal analysis results for a pedestrian bridge are obtained by framing 3 markers for each acquisition, with 2 overlapping markers, between subsequent acquisitions. Then, local mode shapes are extracted for each acquisition and finally, they are stitched together using least-squares fit. With this kind of procedure, mode shapes can be extracted, but the final result is prone to propagation of errors due to possible wrong estimation of local modes, which could influence the final mode shapes found. At the same time, two overlapping markers are always required and this makes the acquisition operations much longer.

In [15], the authors proposed the use of a commercially available drone to measure the displacement of a structure. They performed natural feature tracking to estimate the displacement of the targets and compensate for the motion of the drone by estimating the displacement of background features. The authors identified limitations of the proposed method, including the accuracy of estimation of the camera's motion and the assumption of in-plane motion of the target. In addition, further developments were identified, regarding data fusion techniques with Inertial Measurement Unit (IMU) sensors and measuring of the relative distance between camera and structure. Another approach, described in [16], compensates for camera motion using a distance sensor, by keeping the drone within a limited range of distance from the structure. However, this limited range can reduce the error, but it does not provide a scale factor for each frame. Laboratory studies were presented in [17], regarding the operational modal analysis of a mock-up bridge. This analysis is based on a fixed reference region to be framed in order to obtain the motion of the drone to be compensated for in relation to the vibrations.

A quite different method is presented in [18], where 3D Digital Image Correlation (3D-DIC) is used for modal analysis of a mock-up of wind turbine blades from data acquired from a UAV. In this case, the drone's motion is compensated for by correcting the structure's rigid body motion. However, this method can present a few limitations, such as the use of a speckle patter for 3D-DIC to be applied to structures, correct estimation of the rigid body's displacement, and the ability to stitch together mode shapes of portions of a large structure, that leads to error propagation, as previously described for [13] as well.

In this article, the limitations of the state of the art approaches mentioned are tackled by implementing sensor fusion on a prototype drone. For this purpose, synchronization of the camera on the drone with the fixed camera makes multiple acquisitions of one reference point possible for the fixed camera and many points for the drone camera, with one or more per acquisition. This procedure makes it possible to obtain a modal analysis of a structure without stitching modal shapes from different acquisitions. On the other hand, converting the vibrations from pixels to millimetres is done, knowing the distance between the camera and the target via the ToF sensor. Moreover, the effect of the drone's motion on vibrations is reduced with the trajectory tracking sensor, which returns the drone's trajectory. Furthermore, the measuring points on the structure are identified by knowing the drone's trajectory and the distance of points from the camera, via the ToF sensor. With this method, the issues that are presented in the state-of-the-art articles for measuring vibrations using drones are addressed, resulting in improvements in the vibration measuring results.

III. Proposed Method

The measuring method proposed is defined by data acquisition and post-processing data analysis. The acquisition phase is defined by gathering the following data:

1. Images from the fixed camera of one reference point on a structure.
2. Images from the grayscale camera on the drone to measure the vibrations of specific points on the structure.
3. Depth images acquired via the ToF sensor, to convert vibrations from pixels to millimetres.
4. Trajectory poses acquired from the trajectory tracking sensor, in terms of quaternions and translations, in order to obtain the trajectory of the drone.

The procedure for collecting data using the sensors on the drone is determined by continuous acquisition of the trajectory tracking sensor in order to estimate the trajectory of the drone from the initial point. As for the grayscale and ToF cameras, the drone is moved in front of 1 measuring point and data recording is started to acquire 5000 grayscale camera frames at 142.8 Hz (1 frame every 7 ms, as explained in Section IV.A) and to acquire the corresponding frames of the ToF sensor, at 20 Hz. Multiple points can be measured simultaneously, if they fall within the camera's Field Of View (FOV). Then, the drone is moved to one or more point(s) that follow, and drone system acquisition is repeated and so on, until the last measuring point. For each j-th acquisition of the drone system, synchronized data recording of the fixed camera reference point is performed. This type of synchronization is dealt with as described in Section IV.A. The same procedure is applied for drone and laboratory tests, where the drone measurement system is moved by hand.

A. Data analysis

The analysis of data is composed of the following parts:

1. Calculation of the fixed camera's scale factor (px-mm), by acquiring a flat calibration target, while keeping the camera orthogonal to the target.
2. Correction of grayscale cameras (fixed and drone camera) lens distortion.
3. Tracking of the structure's features by geometric matching [19], in the synchronized images of the fixed and drone grayscale cameras, in order to extract vibration signals, in the plane of the image (the features can be seen as points). Before tracking, histogram equalization [19] was applied to obtain a histogram of the output grayscale image that is flat to exploit the camera's entire measuring range.
4. Synchronization and alignment of the reference systems of the ToF sensor and tracking sensor with the grayscale camera on the drone using software (Section IV.B and Section IV.C).
5. Conversion of the vibration measurements from the drone grayscale camera from px to mm (Section III.B).
6. Compensation for the movement of the drone for the vibrations computed in point 3 for the trajectory returned by the trajectory tracking sensor (Section III.C).
7. Calculation of the auto-spectra and cross-spectra between the reference point measured by the fixed camera and the points measured by the moving camera on the drone.
8. Reconstruction of the 3D geometry of the points measured (Section III.D).
9. Operational modal analysis done using LMS Test.Lab.

All the data analysis parts were executed in post-processing. The main impact on the processing time is due to geometric matching for vibration measurement from grayscale images and the conversion of vibrations from pixels to millimetres, where the alignment and resampling of depth images must be executed for each depth frame, as explained in Section III.B. With these conditions, the processing time is about 15 min using a laptop with an Intel 8-Core i7-7700HQ CPU @ 2.80GHz processor, with 16 GB RAM, for processing one j-th acquisition, composed of 5000 grayscale images from the drone system, with related depth images, and 5000 grayscale images from ground system. Therefore, for the entire modal analysis of 7 marker points (Section IV.D), a total post-processing time of 2 hours was estimated. This processing time can be suitable for post-processing modal analysis. The most critical and innovative parts of the analysis are dealt with in the subsections that follow.

B. Conversion of pixels to millimetres of the drone-mounted grayscale camera images with data from the ToF sensor

Converting the vibration signals obtained from images acquired from the drone from pixels to millimetres, is essential for preserving the correct amplitude ratios of natural frequencies for modal analysis.

Measuring point vibrations are obtained in the plane of the image and a scale factor is required to convert them to millimetres. This conversion is obtained after ToF-grayscale calibration, as described in Section IV.C, using the i-th depth image $I_{i,j}^{d}$ which corresponds to the related i-th grayscale image $I_{i,j}^{g}$ of the j-th grayscale acquisition. The depth of a marker point $d_{i,j}^{p}$ at the i-th grayscale image $I_{i,j}^{g}$ is used to compute the 3D coordinates of the marker, using the following formulae according to the pinhole camera model:

$$\begin{cases} X_{i,j}^{p} = (c_x - x_{i,j}^{p})/f_x * d_{i,j}^{p} \\ Y_{i,j}^{p} = (c_y - y_{i,j}^{p})/f_y * d_{i,j}^{p} \\ Z_{i,j}^{p} = d_{i,j}^{p} \end{cases} \quad (1)$$

where $X^p_{i,j}$, $Y^p_{i,j}$, $Z^p_{i,j}$ are the world coordinates of marker $p^p_{i,j}$, referred to the optical centre of the grayscale camera, $x^p_{i,j}$, $y^p_{i,j}$ are the coordinates of marker $p^p_{i,j}$ in the image plane and c_x, c_y, f_x, f_y are grayscale camera's intrinsic parameters.

The depth value $d^p_{i,j}$ is derived from the depth image $I^d_{i,j}$, by considering the location of the marker detected in the grayscale image $I^g_{i,j}$. A region around the coordinates on the marker is taken to compute $d^p_{i,j}$. The extension of this region is typically that of the templates used for the geometric matching.

C. Drone movement compensation via trajectory tracking sensor

The vibrations measured by geometric matching result in the estimation of the relative displacement between the drone and the target structure. Therefore, the drone's displacement can influence the structure vibration measurements.

For this reason, tracking the displacement of the drone with a specific sensor can improve the quality of results, by isolating the structure's vibrations. To test the feasibility of this concept, a trajectory tracking sensor was added, after calibration and software synchronization with the drone grayscale camera (Sections IV.B-IV.C). This sensor is the Intel RealSense T265. To remove the effect of the drone's movement from vibration measurements, the trajectory returned by the trajectory tracking sensor has to be applied to the 3D points computed in equation (1). This trajectory is defined in the reference system of the Intel RealSense T265 sensor and calibration matrices have to be used to consider the trajectory of grayscale camera. The new 3D point $p^c_{i,j}$ with drone movement removal is obtained, as in the following equation:

$$p^c_{i,j} = \left(\left[T_{p-imu}\right] * \left[T_{imu-g}\right]\right) * \left[T_{T265,\mathrm{i,j}}\right]' * \left(\left[T_{p-imu}\right] * \left[T_{imu-g}\right]\right)^{-1} * p^p_{i,j} \qquad (2)$$

where $p^p_{i,j}$ is the point expressed as in equation (1) in homogenous coordinates, $\left[T_{imu-g}\right]$ is the homogenous matrix to pass from the T265 IMU to the grayscale camera reference system and $\left[T_{p-imu}\right]$ is the homogenous matrix to pass from the T265 pose to the T265 IMU reference system, given by T265 calibration, provided by the manufacturer [20]. The matrix $\left[T_{T265,\mathrm{i,j}}\right]'$ is directly the homogenous matrix returned by the T265 sensor, expressed as the i-th pose of the sensor of the j-th acquisition. This matrix is obtained after removing the initial offset of the T265 sensor's trajectory, using the following equation:

$$\left[T_{T265,\mathrm{i,j}}\right]' = \left[T_{T265,\mathrm{1,j}}\right]^{-1} * \left[T_{T265,\mathrm{i,j}}\right] \qquad (3)$$

With these considerations, vibration measurements can be improved with a reduction of drone movement effect.

D. Reconstruction of the structure's geometry using a trajectory tracking sensor

Another advantage of having defined the 3D measurement points, as in eq. (2), and of having a trajectory tracking sensor is the possibility to reconstruct the 3D geometry of the structure being tested.

The 3D geometry can be extracted by looking at 2 contributions: one given by the trajectory returned by the T265 sensor and the other by the location of the markers in relation to the grayscale reference system $p^c_{i,j}$. The location of the markers is determined as the mean of the position of markers in the j-th acquisition p^c_j of all the i-th positions $p^c_{i,j}$, in relation to the grayscale camera reference system. Following the same principle, the T265 sensor position is retrieved by computing the mean $[T_{j,T265}]$ of all the i-th poses $[T_{i,j,T265}]$ of the T265 sensor, during j-th acquisition. The poses are defined by homogenous matrices. In this case, for the sake of convenience, the trajectory of the T265 is not transported to the grayscale camera reference system, but the location of markers is referred to the reference system of the T265. The trajectory of the drone, identified by sensor T265, relates to reference systems at j-th acquisitions locations. On the other hand, the 3D geometry of the structure is calculated using the following expression:

$$p^c_{T265,j} = \left[T_{T265,\mathrm{j}}\right]' * \left(\left[T_{p-imu}\right] * \left[T_{imu-g}\right]\right) * p^c_j \qquad (4)$$

With this procedure, it is possible to reconstruct the 3D geometry of the structure being inspected.

E. Operational Modal Analysis

Operational modal analysis (OMA) aims to identify the modal parameters, such as natural frequencies and mode shapes of a structure, only from the vibration data collected when the structure is under artificial or natural excitation. Of the software available for OMA, one well-known algorithm is PolyMAX [21], that is largely used for estimating structure parameters from vibration measurements. The method can be implemented as a least-squares complex exponential method: in a first step a stabilisation diagram is constructed containing frequency, damping and participation information. Next, the mode shapes are selected among the stable poles. One of the specific advantages of the technique lies in the very stable identification of the system poles [21]. This algorithm can take the cross-spectra of points of a structure with the 3D geometry as input to reconstruct mode shapes, as it was done in this study. This algorithm was also used successfully for analysis similar to that presented in this article [18]. Furthermore, the comparison of mode shapes, between those obtained using accelerometers and the proposed method, was handled with the Modal Assurance Criterion (MAC), that is a well-known technique for comparing mode shapes [22]. This criterion is expressed by an indicator to show the similarity between modes computed using cameras and accelerometers (Section V.B). The modal analysis techniques described in this section are used as tools, since the main novelty of this article is the proposed measurement technique to obtain data to apply modal analysis.

IV. Experimental Setup and Validation

The measuring system is composed of a grayscale camera (Flir Blacfkfly BFS-U3-16S2M) fixed on a tripod (fig. 2.a) and a system mounted on a prototype drone (fig. 2.b-2.c) composed of a grayscale camera (Flir Blacfkfly BFS-U3-16S2M), Basler Blaze 101 ToF sensor and Intel RealSense T265 tracking sensor. The grayscale cameras, one fixed and the other on the drone, are synchronized by a trigger transmitted via RF transceivers (Section IV.A). The sensors of the system on the drone (grayscale camera, Basler Blaze 101 and Intel RealSense T265) are synchronized via software (Section IV.B) and they are calibrated to align all data to the same reference system (Section IV.C). The selection of the Basler Blaze 101 sensor is based on the sensor's ability to work outdoors as well, since it works at 940 nm, at which daylight has a drop and does not interfere with the sensor [4]. The accuracy and precision of this ToF sensor are +/- 5mm and 0-2 mm, respectively, as expressed by the manufacturer, in indoor conditions [23] and of +/- 7 mm and 5 mm, respectively, for outdoor conditions [4]. This uncertainty level is suitable for our application, since to convert vibration measurements from px to mm, the error on X and Y direction caused by distance measurement error would be a percentage of the distance measurement error with respect to the sensor to target distance, e.g. 10 mm error over 1000 mm of sensor to target distance, corresponding to an uncertainty of 1% on the scaling factor. This consideration can be derived from eq. 1. On the other hand, the Intel RealSense T265 sensor was added to this system since it represents an affordable sensor for tracking the trajectory of the drone, making it a good option for a feasibility study.

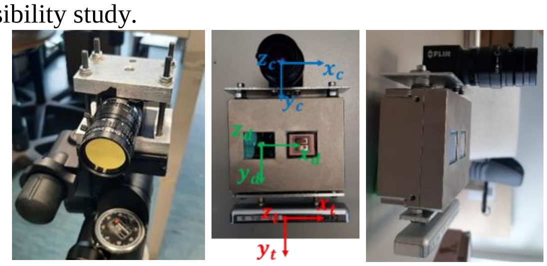

(a) (b) (c)

Fig. 2 – The measurement system: fixed grayscale camera (a), drone measurement system, front-view with layout of sensors reference systems (b) and profile view (c)

A. Grayscale cameras synchronization

Synchronization of the drone grayscale camera and the fixed grayscale camera is based on 3 nrf24l01 transceivers, used to send triggers via radio frequencies at 2.4 GHz. The layout of the transmission of triggers data is given in fig. 3.a, while the device to be used on the drone can be seen in fig. 3.b, and only weighs 25.3 g. One device is used as a transmitter of a series of trigger pulses and the other two are used as receivers, one for the drone camera and the other for the fixed camera. Each receiver is connected to an Arduino Nano, to make the system more compact and lightweight. The transmitter sends a series of pulses to both receivers, and both microcontrollers connected to receivers generate a trigger when a pulse is obtained by the receivers. The information sent by the transmitter is the trigger number, starting from 1 to the last. After transmission of all the triggers, one of the receivers sends the number of the first trigger received back to the transmitter and later, the second receiver sends the same information, as well. With this method, the number of the first trigger received is known, for both receivers.

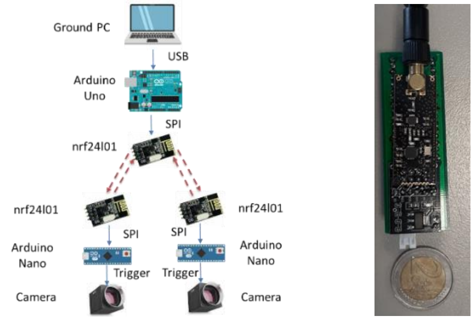

(a) (b)

Fig. 3 – Layout of RF triggers transmission (a) and the device to be assembled on the drone (b)

This system was tested by measuring the trigger signal as a digital input at 5V, generated by both microcontrollers and going to the cameras, using a National Instruments NI 9402 acquisition board, at 1000 kS/s. The delay between a trigger sent to both cameras was estimated to be 13.3 µs (RMS of the delay). The triggers' frequency was set to obtain 1 sample over 7 ms, corresponding to 142.8 Hz, that was estimated to be the best choice for the camera exposure time, trigger width and measurement frequency range required. Therefore, the delay between the two triggers is negligible compared to the measured frequency range. An analogous approach with similar uncertainty results is also described in [24].

B. ToF camera, tracking camera and grayscale camera synchronization

To process the data gathered from 3 different types of sensors, a synchronization procedure is required to have all data of sensors on the drone, referred to the same timestamps. The 3 sensors are acquired using a multi-thread approach, with the grayscale camera running on a different core, from the other sensors, to guarantee the FPS required for the grayscale camera. FLIR, Basler Blaze 101 and Intel RealSense T265 sensors are acquired at 142.8, 20, and 200 Hz, respectively. The series of timestamps taken as a reference is that one of the grayscale camera, since it is the one used to measure vibrations. Time synchronization can only be executed using software, since it is not possible to send a trigger to the Basler Blaze 101 and to the Intel RealSense T265, according to documentation [25][26]. Therefore, only software synchronization can deal with these sensors.

As for the Intel RealSense T265 sensor, the synchronization is given by a simple interpolation of data, coming from the Intel RealSense T265 sensor, to obtain the same timestamps as the grayscale camera. This method is similar to the one used in [27], where the closest pose from the Intel RealSense T265 is assigned to the frame of the other camera. This interpolation is justified by the higher sampling frequency of the Intel RealSense T265.

Regarding Basler Blaze 101 sensor, an interpolation of data is performed using the same method as for the Intel RealSense T265 sensor, with the difference of extracting the distance of markers and interpolating that distance. The Basler Blaze 101 sensor is acquired at 20 Hz and the interpolation is justified by the quasi-static condition of the drone, when the measurement is performed, with the drone being in hovering mode and with no significant speed or acceleration. Therefore, only small variations in the distance between the drone and the target are expected while measuring vibrations.

C. ToF camera, trajectory tracking sensor and grayscale camera calibration

The measurement system on the drone must be calibrated, in order to have all the data from all sensors referred to the reference system of the grayscale camera.

The alignment of the reference systems of a ToF sensor (Basler Blaze 101) and a grayscale camera has already been dealt with in literature and it is given by a stereo camera calibration, that makes it possible to obtain homogenous transformation between the two cameras, as described in [28]. The same procedure was applied in this article. Depth images that correspond to the related grayscale images with the same resolution are obtained by resampling the point clouds of depth images, using the method described in [29].

As for the Intel RealSense T265 sensor, this sensor is composed of 2 fisheye cameras and an IMU, with an internal processing unit that operates trajectory tracking algorithms as Simultaneous Localization and Mapping (SLAM), to provide tracking of the position of the sensor itself. The transformation required to pass from the T265 pose reference system to the T265 IMU reference system is provided by the manufacturer, according to documentation [20]. To pass from the T265 IMU reference system to the grayscale camera reference system, IMU-camera calibration described in [30][31] was applied. These calibration procedures are well known in literature. This specific method takes the images of a target framed by the camera and the signals returned by the IMU, in order to identify the trajectory of both sensors and to find the transformation between the IMU and the camera. These calibration algorithms are not discussed in detail in this article, since they are already present in literature [30][31].

D. Benchmark structure description

In order to validate the proposed vibration measurement approach, a mock-up structure was built. This structure is based on an 3000x2000 mm L-shaped beam, as shown in the scheme in fig. 4. This structure is made of an aluminium beam with a 30x30 mm cross section. The location of accelerometers is visible in fig. 4, with positions in relation to the reference system for the structure. The structure is connected to the ground with springs, in order to simulate a free-free beam. The structure is excited by a shaker placed in position 1, in fig. 4. The connection between the shaker and the beam is formed by a spring. The excitation is generated using a white noise signal with a frequency range of approximately 0-70 Hz, in order to cover the spectrum measured by cameras up to the Nyquist frequency (142.8 FPS). Accelerometers are placed in the same positions as the markers to measure the vertical vibration and to make a comparison with the results given by the proposed method. The fixed camera frames the marker in position 1, while the drone frames the other markers. An example of a marker is visible in fig. 4. It is based on a screw in the required position, to simulate a possible mechanical joint that can be present in a real structure. For space reasons, the lab tests were performed using a handheld camera framing the internal side of the L beam while, during the drone test, the drone framed the outer side of the L beam.

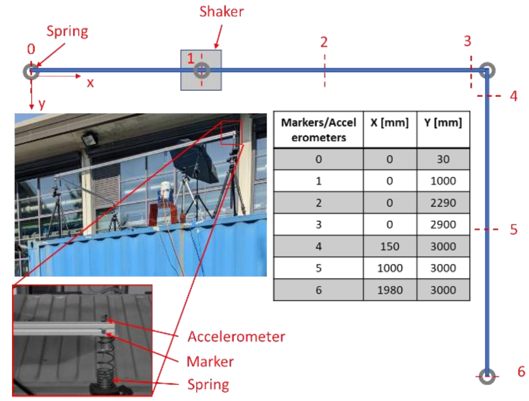

Fig. 4 – Scheme of the structure being inspected with geometry and position of markers, accelerometers and shaker

E. Prototype Drone description

The prototype drone used for the experiments is composed of a Tarot T960 frame with 6 Tarot 5008-340 kv brushless motors. The payload, that the drone can actually lift, is 2–3 kg of additional weight and the autonomy is about 20 min, extended by a tethering cable used to power the drone from the ground. The flight controller is a PixHawk PX4, that is accessible for getting data from its sensors. This type of configuration is flexible making it possible to assemble different sensors. The acquisition is done by saving data on a LattePanda 864s board, the memory of which was enlarged by adding an SSD memory board. The prototype drone can be seen in Fig. 5, during acquisition.

Fig. 5 – Prototype Drone

V. Results and Discussion

The results were obtained both in the laboratory with the drone measuring system moved by hand to simulate drone acquisition and outdoors using the prototype drone. However, the results are presented in order to highlight the innovative improvements of vibration measurement using drones and to identify the measurement quality, obtained with this research. In particular, these improvements relate to:

1. Compensation of the drone's vibrations to reduce the impact of the drone on vibration measurement.
2. Modal analysis from drones.
3. The 3D geometry of the structure to be used for modal analysis.

An example of the modulus of a cross-spectrum, calculated using data from accelerometers, is visible in fig. 6. There are 6 resonance frequencies: the first three (4.4, 6.2, 7.5 Hz) relate to the presence of springs connecting the structure to the ground (fig. 4) and the last three are natural frequencies of the structure (15.6, 31.3, 43.3 Hz). The latter frequency could not be detected during drone tests, due to low amplitudes of frequencies that are lower than the noise level for both fixed and drone cameras in terms of displacements, as discussed in Section V.B.

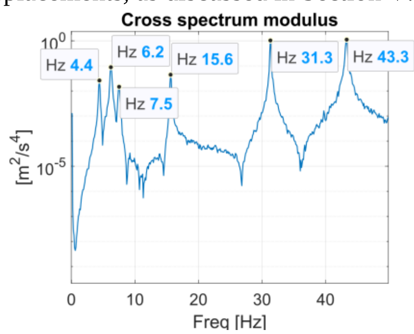

Fig. 6 – Example of a cross-spectrum calculated from accelerometer data on the structure being inspected

A. *Compensation of drone vibrations*

The presence of the trajectory tracking sensor makes it possible to track the trajectory of the drone. One possible application of the T265 is tracking a drone trajectory, according to documentation [26]. This information could be useful for the purposes of this research, for removing the effect of the drone's motion on vibration measurements.

The results of this compensation are visible in fig. 7, where fig. 7.a-7.b-7.c are associated with the lab test and fig. 7.d-7.e-6.f with the drone test, for fixed and moving cameras (handheld or on drone) for markers 1 and 5, respectively. For both lab and drone tests, drone vibration compensation leads to a reduction in noise level, in particular in the frequency range below 20 Hz. This reduction is clearer for auto-spectra in fig. 7.c-7.d. This improves the ability to detect resonance frequencies, especially those at lower frequencies. This reduction can be helpful to identify modes at frequencies lower than 20 Hz, that are quite common for the first modes of civil engineering structures. The lower level of noise is also demonstrated by the RMS of the auto-spectra, computed between 0.2-20 Hz, shown in Table 1. As can be observed, the RMS is reduced by at least 4 times for each marker. The RMS was computed for all markers, except for marker 1, that was only framed by the ground camera. This reduction helps to identify frequencies below 20 Hz, while higher frequencies are less affected by the movement of the drone and they could not be compensated using the tracking sensor data. The RMS in Table 1 is not considered for frequencies lower than 0.2 Hz to exclude the value at 0 Hz, which represents the static component of the signal.

TABLE I – RMS OF MARKER SIGNALS FRAMED BY THE DRONE SYSTEM

Marker	0	2	3	4	5	6
No trajectory compensation	9.16	9.81	16.2	15.3	16.7	8.46
Trajectory compensation	1.36	1.37	3.69	2.14	2.27	2.00

It is also important to note that frequencies at 15.6 Hz, 31.3 Hz and 43.3 Hz are not visible in the auto-spectrum of the drone camera (fig. 7.d). This is caused by the higher noise level due to the drone's movement, for which the compensation is not precise enough to reduce noise under 10^{-4} mm^2. However, in cross-spectra (fig. 7.e-7.f), computed between reference marker 1 and marker 5, resonance frequencies at 15.6 Hz and 31.3 Hz are easy to identify, since the uncorrelated noise between the vibrations of markers 1 and 5 is not present in cross-spectra. The same consideration applies to the first 3 modes (4.4-6.2-7.5 Hz). On the other hand, the frequency of the mode at 43.3 Hz is clearly identified for the laboratory test, while it is affected by noise for the case of the drone test, for fixed camera measurements as well (fig. 7.b) and, therefore, the mode shape at that specific frequency could not be reliably reconstructed. This is probably caused by the drone's air flow affecting the structure's vibrations while also disturbing the fixed camera. To conclude, the compensation of the drone's movement on vibration measurements is effective between 0-20 Hz, while it is not particularly relevant at higher frequencies. This reduction can be important for identifying vibration modes at low frequencies, that are typical of civil structures.

With these results, we observed that the noise in the cross-spectrum of drone tests in fig. 7.f is around 10^{-4}-10^{-5} mm^2, for frequencies higher than 10 Hz and around 10^{-2} mm for frequencies lower than 10 Hz. Therefore, this system is suitable for structures with displacements of tenths of millimetres, even though in a frequency range from 10 Hz up to the Nyquist frequency, the minimum mode amplitude that can be detected is around hundredths of millimetres. These results were reached by keeping a distance between the grayscale camera on the drone and the target of between 1 and 2 m.

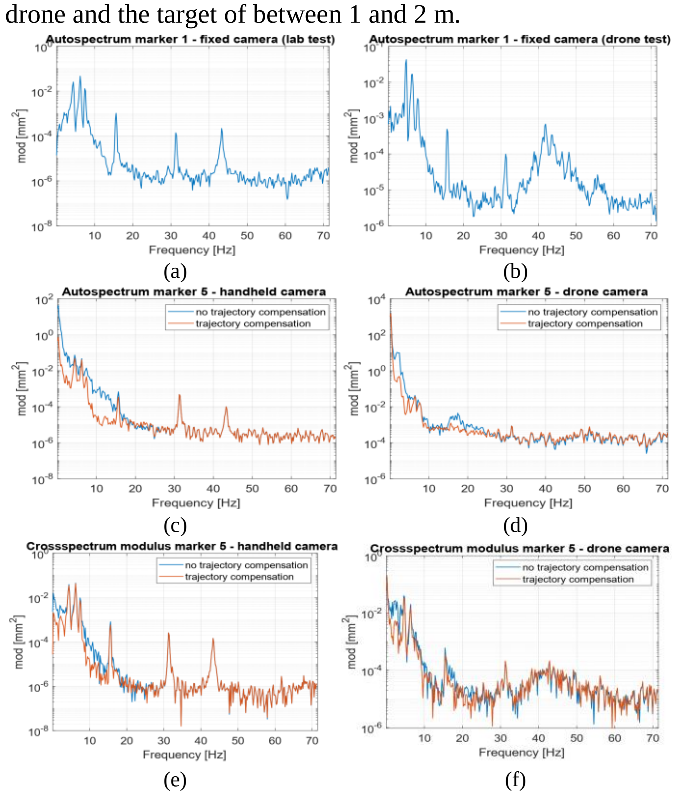

Fig. 7 – Compensation of the movement of the drone: auto-spectra of marker 1 from fixed-camera data (a-b), auto-spectra of marker 5 from drone camera (c-d), cross-spectra between markers 1 and 5 (e-f). A-c-e are from lab test, b-d-f from drone test

B. *Modal analysis results*

The modal analysis results were obtained using LMS Test.Lab software and they are reported in terms of resonance frequencies and mode shapes. As already explained in section V, only during the drone test, it was not possible to identify the structure's last natural frequency (43.3 Hz). This is probably caused by the rotation of the drone blades, that increases the noise level between 40 to 50 Hz (fig. 7.f). For markers 3 and 4 (fig. 4), histogram equalization pre-processing was required before tracking the markers. In particular, this algorithm is based on transforming the input grayscale image to obtain a histogram of the output grayscale image that is flat. This method makes it possible to exploit the camera's entire measurement range and to reduce the effect of lighting conditions. All markers were tracked and the results are reported.

Tables I and II show the detected poles after LMS Test.Lab modal analysis measured by accelerometers and by the proposed measuring system and method, for the laboratory test (Table I) and for the drone test (Table II). As can be seen, the frequencies measured by accelerometers and camera are very close, since the difference on average is 0.28 % and 0.26 % of the frequencies measured using accelerometers (corresponding to 0.018 and 0.036 Hz).

TABLE I – STRUCTURE FREQUENCIES – LAB TEST

Mode number	**Acc. Freq. [Hz]**	**Cameras Freq. [Hz]**	**Freq. Diff. [Hz]**
1	4.39	4.42	0.03
2	6.25	6.22	0.03
3	7.48	7.47	0.01
4	15.60	15.62	0.02
5	31.30	31.29	0.01
6	43.25	43.26	0.01

TABLE II – STRUCTURE FREQUENCIES – DRONE TEST

Mode number	**Acc. Freq. [Hz]**	**Cameras Freq. [Hz]**	**Freq. Diff. [Hz]**
1	4.77	4.78	0.01
2	6.29	6.33	0.04
3	7.73	7.73	0.00
4	15.62	15.61	0.01
5	31.33	31.21	0.12

The reconstruction and identification of mode shapes using the proposed method is validated by direct comparison with mode shapes obtained using accelerometers, that were placed in the same positions as the markers.

As explained in Section III.E, the comparison of mode shapes was handled applying the Modal Assurance Criterion (MAC), shown in Tables III and IV, respectively. By looking at the data, it is possible to conclude that all modes detected by cameras can be correctly linked back to the correct vibration modes. This confirms that it is possible to retrieve the correct mode shapes using the proposed method. In few cases, the drone mode shapes can be closer to accelerometers ones with respect to laboratory results. This can be caused by closer resonance peaks ratios with respect to accelerometers, even if with drone tests the resonance mode shape at 43 Hz could not be identified for the noise caused by the rotation of drone blades. In addition, the increase of the noise level introduced in the drone measurements is visible in the autospectra and cross-spectra in fig. 7.d and 7.f, with respect to the lab measurements in fig. 7.c and 7.e. This noise level is about 10^{-5}-10^{-6} for lab tests and about 10^{-4} for drone measurements.

TABLE III – MAC LAB

		Accelerometers					
	Modes	**1**	**2**	**3**	**4**	**5**	**6**
Cameras	**1**	**81.7**	0.61	1.62	3.11	4.05	6.97
	2	3.70	**87.3**	15.8	12.0	14.6	6.41
	3	0.78	15.6	**78.1**	2.33	9.55	1.03
	4	0.10	4.36	2.67	**78.5**	2.80	23.4
	5	29.5	1.19	8.87	1.28	**77.8**	3.09
	6	1.71	0.75	0.19	6.21	0.36	**92.6**

TABLE IV – MAC DRONE

		Accelerometers				
	Modes	**1**	**2**	**3**	**4**	**5**
Cameras	**1**	**91.4**	0.29	8.42	7.53	11.8
	2	0.56	**83.7**	9.12	6.36	2.91
	3	0.06	16.6	**86.9**	4.04	9.37
	4	1.62	11.4	4.66	**91.9**	1.12
	5	6.79	2.02	10.0	2.89	**80.4**

In addition, the mode shapes measured at the marker locations can be seen in fig. 8. These mode shapes were normalized in relation to the reference marker amplitude and computed directly using LMS Test.Lab. As expected, the mode shapes are closer between accelerometers and cameras, where the MAC indicator is larger and modes are more similar (modes 1 and 5 for drone test, fig. 8). However, the amplitudes of modes can present differences for drone tests, as shown in fig. 8. This aspect can be relevant in terms of identification of defects and structural changes. Therefore, to summarize, this measurement technique can be used to identify frequency changes up to 0.2-0.3 % and, with the tests presented in this article, there should be a relevant change in mode shapes that prevents associating the measured modes with those measured in standard conditions, using MAC indicators. Indeed, only a significant reduction in the MAC indicator for correlated modes would be meaningful in terms of changes in mode shapes. Further investigations are needed to determine the uncertainty of the system in reconstructing mode shapes, in order to determine the fault level can be detected using this technique. However, in this article, a feasibility study is presented in order to perform modal analysis using drones and these results prove our system's ability to identify and reconstruct modes and, potentially, to identify possible changes in structures that would suggest significant damage or defects.

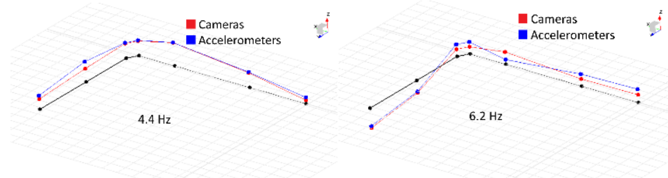

(a) (b)

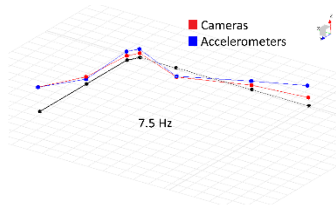

(c)

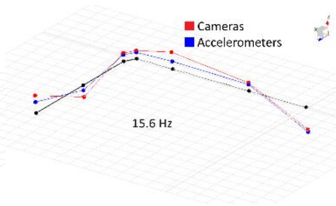

(d)

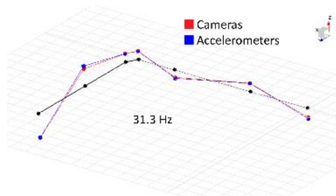

(e)

Fig. 8 - Mode shapes from mode 1 to 5 (a-e) measured by cameras and accelerometers for drone tests. The undeformed geometry is given in black in the graphs.

C. *Reconstruction of the 3D geometry of the structure*

The 3D geometry of the measured points must be known in order to perform modal analysis. This geometry has to be measured using other techniques in the case of modal analysis involving accelerometers, while when using drones the position of markers would be more difficult to extract, in the case of large structures.

In fig. 9, reconstruction of the 3D geometry is shown in red, for both the laboratory (fig. 9.a) and the drone test (fig. 9.b). As can be seen, the drone's trajectory is represented by the blue line and by the reference systems, described by the homogenous matrix $[T_{j,T265}]$, as written in Section III.D. The expected 3D geometry is as represented by the scheme in fig. 4. By looking at fig. 9, the 3D geometry can be clearly identified, for both the lab and the drone tests, with the difference that for the drone test the geometry is inclined in relation to the trajectory. This is related to the assembly of the measuring system, that, on the drone, has a certain slope in relation to the ground (about 14°), to avoid getting the drone blades in the frame.

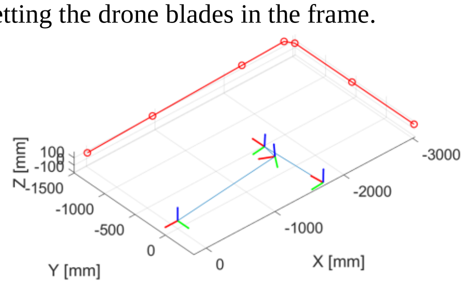

(a)

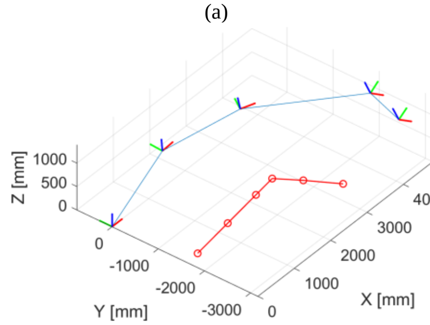

(b)

Fig. 9 – 3D geometry reconstruction of the structure, in red, and 3D trajectory of the drone, in blue, with reference system representations, for lab test (a) and drone test (b)

In this case, it was observed that drone vibrations have a limited effect on the 3D reconstruction of the target structure, since they act at a frequency range that is not close to the translation of the drone to pass from one marker to another. Moreover, the contribution of the ToF sensor with the trajectory tracking sensor can provide the scale factor and the target distance from the drone for every frame acquired.

On the other hand, the tracking sensor can have a strong impact on the 3D reconstruction of the target structure uncertainty. The structure vibrations do not influence the tracking sensor, since the fisheye cameras in Intel RealSense T265 sensor are not pointing at the structure, but they are directed downwards. Moreover, the use of fisheye cameras allows to track more accurately the drone trajectory, since there is a reduction of the drift that would be caused by the usage of only IMU data. A more quantitative evaluation can be done in terms of the average distance difference between true ground marker coordinates and those computed using the system being evaluated. The coordinates relate to the reference system in fig. 4. Another relevant indicator is the error in terms of estimating the total length of the beam being inspected. In this case, the reconstruction given by the drone test is less accurate than the laboratory tests, since the markers' distance to the true ground is 39.5 mm and 138.8 mm, for lab and drone tests, respectively. In the same way, the total beam length differs in relation to the true ground by 1.25% and 11.40%, for lab and drone tests, respectively. However, these results comply with the performance of the T265 sensor [32], that can have trajectory errors of between 0-20% in the case of a low number of features for the T265 sensor to track. The authors are aware that the level of uncertainty may not be consistent with the final application. This depends mainly on how accurate the 3D points should be placed in the 3D geometry. However, since this is a feasibility study, the major point dealt with in this article is the ability to perform modal analysis using a drone with the system being evaluated. For higher trajectory tracking precision, other more expensive systems could be applied. However, this research made it possible to demonstrate that the 3D geometry of a structure can be obtained by correctly tracking the drone's trajectory and by knowing the position of markers, in relation to the grayscale camera, using the procedure explained in Section III.D. This result shows that this type of 3D geometry reconstruction is feasible and more advanced equipment would be more effective in determining the structure's geometry.

VI. Conclusions

In this article, the feasibility of performing modal analysis using drones was investigated. In particular, the main challenges in this field are (i) modal analysis performed using drones, (ii) conversion of resonance vibration amplitudes from pixels to millimetres, (iii) compensation of drone movements to isolate the structure's vibrations in relation to the drone's displacement and (iv) 3D geometry reconstruction of the measurement points. The first issue was tackled by using a ToF sensor to measure the distance between the grayscale camera and the target, while drone movement mitigation and 3D geometry were obtained by using a trajectory tracking sensor that returned the drone's movements.

The results proved that it is possible to reliably measure the resonance frequencies with an error of 0.2-0.3 %, while the mode shapes can be reconstructed effectively. It was also observed that the modes could be correctly recognized and with the MAC indicator it was possible to correlate each camera mode with the corresponding accelerometer mode. The MAC indicator for corresponding modes was always higher than 80%, for drone tests. Furthermore, 3D geometry reconstruction of the measured points was performed as well, even if there is a significant reduction in performance in outdoor drone tests. To improve the results in terms of mode shapes and 3D geometry reconstruction, more reliable drone trajectory tracking methods could be used, e.g. Real-Time Kinematics (RTK) in order to reduce drifts in drone translation estimations. In addition, it worth considering that the tests were carried out without a gimbal on the drone and, thus, in a more critical condition in terms of drone vibrations.

References

[1] Ham Y., Han K.K., Lin J.J., Golparvar-Fard M., "Visual monitoring of civil infrastructure systems via camera-equipped Unmanned Aerial Vehicles (UAVs): a review of related works", *Visualization in Engineering*, Volume 4, Issue 11 December 2016

[2] Fan W., Qiao P., "Vibration-based damage identification methods: A review and comparative study," *Struct. Health Monitor.*, vol. 10, no. 1, pp. 83–111, Jan. 2011.

[3] Feng D., Feng M. Q. "Computer vision for SHM of civil infrastructure: From dynamic response measurement to damage detection – A review", *Engineering Structures*, Volume 156, Pages 105 - 1171 February 2018

[4] Marchisotti D., Zappa E., "Feasibility Study of Drone-Based 3-D Measurement of Defects in Concrete Structures", *IEEE Transactions on Instrumentation and Measurement*, Volume 71, 2022

[5] Cha Y.-J., Choi W., Büyüköztürk O., "Deep Learning-Based Crack Damage Detection Using Convolutional Neural Networks", *Computer-Aided Civil and Infrastructure Engineering*, Volume 32, Issue 5, Pages 361 – 378, May 2017

[6] Peeters B., Ventura C.E., "Comparative study of modal analysis techniques for bridge dynamic characteristics", *Mechanical Systems and Signal Processing*, Volume 17, Issue 5, Pages 965 – 988, September 2003

[7] Zonzini F. et al, "Vibration-Based SHM with Upscalable and Low-Cost Sensor Networks", *IEEE Transactions on Instrumentation and Measurement*, Volume 69, Issue 10, Pages 7990 – 7998, 2020

[8] Favarelli E., Giorgetti A., "Machine Learning for Automatic Processing of Modal Analysis in Damage Detection of Bridges", *IEEE Transactions on Instrumentation and Measurement*, Volume 70, 2021

[9] Bocca M., Eriksson L. M., Mahmood A., Jäntti R., Kullaa J., "A synchronized wireless sensor network for experimental modal analysis in structural health monitoring", *Computer-Aided Civil and Infrastructure Engineering*, Volume 26, Issue 7, Pages 483 – 499, October 2011

[10] Araujo A. et al, "Wireless measurement system for structural health monitoring with high time-synchronization accuracy", *IEEE Transactions on Instrumentation and Measurement*, Volume 61, Issue 3, Pages 801 – 810, March 2012

[11] Seo J., Duque L., Wacker J., "Drone-enabled bridge inspection methodology and application", *Automation in Construction*, Volume 94, Pages 112 – 126, October 2018

[12] Lavatelli A., Balcaen R., Zappa E., Debruyne D., "An Experimental Investigation on Uncertainty in Measuring Vibration Deflection Shapes with Digital Image Correlation", *IEEE Transactions on Instrumentation and Measurement*, Volume 69, Issue 6, Pages 2826 – 2836, June 2020

[13] Hoskere V., Park J.-W., Yoon H., Spencer B.F., "Vision-Based Modal Survey of Civil Infrastructure Using Unmanned Aerial Vehicles", *Journal of Structural Engineering*, Vol. 145, Issue 7, July 2019

[14] Lavatelli A., Zappa E., "Modeling Uncertainty for a Vision System Applied to Vibration Measurements", *IEEE Transactions on Instrumentation and Measurement*, Volume 65, Issue 8, Pages 1818 – 1826, August 2016

[15] Yoon H., Shin J., Spencer B. F., "Structural displacement measurement using an unmanned aerial system", *Computer-Aided Civil and Infrastructure Engineering*, Vol. 33, 2018, pag. 183–192

[16] Herrman R., Moortgat-Pick A., Marx F., "Vibration Analysis of Structures using a Drone (UAV) based Mobile Sensing Platform", SMAR 2019

[17] "Three-Dimensional Reconstruction-Based Vibration Measurement of Bridge Model Using UAVs"

[18] Khadka A., Fick B., Afshar A., Tavakoli M., Baqersad J., "Non-contact vibration monitoring of rotating wind turbines using a semi-autonomous UAV", *Mechanical Systems and Signal Processing*, Volume 138, 2020

[19] Gonzalez R., Woods R., "Digital Image Processing", *Pearson*, 4th edition March 20, 2017

[20] Intel RealSense T265 reference system documentation: https://github.com/IntelRealSense/librealsense/blob/master/doc/t265.md (Last access date: Sept 26th 2022)

[21] Peeters B., Van der Auweraer H., "PolyMAX: A revolution in operational modal analysis", *1st International Operational Modal Analysis Conference*, IOMAC 2005, 2005

[22] Allemang R. J. "The Modal Assurance Criterion (MAC): Twenty Years of Use and Abuse", *Proceedings of SPIE - The International Society for Optical Engineering*, Volume 4753 I, Pages 397 – 405, 2002

[23] Basler Blaze 101 accuracy and precision documentation: https://docs.baslerweb.com/accuracy-and-precision, (Last access date: Apr 18th 2023)

[24] Kauhanen H., Rönnholm P., "Wired and wireless camera triggering with Arduino", *ISPRS Archives*, Volume 42, Issue 3, Pages 101 – 106, October 2017

[25] Basler Blaze 101 documentation: https://docs.baslerweb.com/blaze-101 (Last access date: Sept 26th 2022)

[26] Intel RealSense T265 documentation: https://dev.intelrealsense.com/docs/tracking-camera-t265-datasheet (Last access date: Sept 26th 2022)

[27] Tsykunov E., Ilin V., Perminov S., Fedoseev A., Zainulina E., "Coupling of localization and depth data for mapping using Intel RealSense T265 and D435i cameras", arXiv:2004.00269, 2020

[28] Franco J.M., Caicedo J.M., Marulanda J., Sutton, Sutton M., Thomson P., "RGB-D-DIC technique for low-cost 3D displacement fields measurements", *Engineering Structures*, Volume 197, October 2019

[29] Marchisotti D., Zappa E., "Virtual simulation benchmark for the evaluation of simultaneous localization and mapping and 3D reconstruction algorithm uncertainty", *Measurement Science and Technology*, Volume 32, Issue 9, 2021

[30] Furgale P., Rehder J., Siegwart R., "Unified Temporal and Spatial Calibration for Multi-Sensor Systems", *IEEE/RSJ International Conference on Intelligent Robots and Systems (IROS)*, 2013, Tokyo, Japan

[31] Furgale P., Barfoot T.D., Sibley G., "Continuous-Time Batch Estimation Using Temporal Basis Functions", *IEEE International Conference on Robotics and Automation (ICRA)*, 2012, pp. 2088–2095, St. Paul, MN

[32] Hausamann P., Sinnott C. B., Daumer M., MacNeilage P. R., "Evaluation of the Intel RealSense T265 for tracking natural human head motion", *Scientific Reports*, Volume 11, Issue 1, December 2021

Daniele Marchisotti is a PhD student at the department of mechanical engineering of Politecnico di Milano. He received his MSc degree in Mechanical Engineering. His research interests involve vision-based measurements with RGBD sensors in dynamic environments, such as on drones.

Emanuele Zappa (M'10, SM'21) is full professor in Mechanical and Thermal Measurements at Politecnico di Milano, Italy. He is Associate Editor in Chief of IEEE Transaction on Instrumentation and Measurement. His scientific activity is mainly in the field of mechanical and image-based measurement.